doi: 10.1109/ICSENS.2011.6127268

A Scalable CMOS Sensor Array for Neuronal Recording and Imaging

Ben Johnson*, Shane T. Peace†, Thomas A. Cleland‡, and Alyosha Molnar*
*School of Electrical and Computer Engineering
†Department of Neurobiology and Behavior
‡Department of Psychology
Cornell University
Ithaca, NY 14850
Email: bcj25@cornell.edu

***Abstract*— We present a CMOS sensor array with 768 low-noise recording sites for neural recording with 2,048 intercalated angle-sensitive pixels (ASP) for optical read-out. The design is highly scalable due to electrode-level digitization with serial data stream-out. The front-end amplifiers use chopping to reduce flicker noise and achieve an input-referred noise of 4.1μV_{rms} over a 4.2kHz bandwidth while occupying an area of only 800μm^2. Digitization is performed by using a distributed ramp ADC that samples every sensor site at 10kHz. Each electrode is plated with platinum to increase the interface capacitance and ensure biocompatibility. The large number of electrodes, 50μm electrode-pitch, and combined optical information will enable sophisticated optogenetic neurophysiological research on a chip.**

I. Introduction

How networks of neurons work together to perform complex tasks and propagate information is an active area of research. To effectively study neural ensembles, neurophysiologists employ microelectrode arrays (MEA) to simultaneously acquire electric field activity across relatively large areas of tissue. The advantages of increasing the number of recording electrodes include: 1) the possibility for a greater number of single cell recordings and 2) spatially broad analysis of local field potentials (LFPs) that can provide insights into how and why neuronal ensembles synchronize their activity. MEA data is an invaluable resource for computational neuroscience and to study biological learning, acute and chronic drug effects, and physiological disorders.

Recording neural signals requires low-noise instrumentation. Extracellular biopotentials typically range in amplitude from 10μV to about 5mV, with power in the 10-200Hz band for LFPs and 200Hz-5kHz band for action potentials[1]. Studies at Cornell University of 300μm thick mouse olfactory bulb slices with MEAs have observed synchronous LFPs that span over 600μm laterally while spiking activity from individual cells typically spreads less than 100μm. Thus, a useful planar MEA should have an active area larger than 1mm on a side to accommodate an entire slice and have an electrode pitch of less than 100μm to fully sample extracellular potentials. Most commercially available MEAs are fabricated on passive, patterned substrates which use off-substrate amplifiers (Multichannel Systems; Ayanda-Biosystems). While these MEAs typically have between 60-256 electrodes, passive routing limits the electrode scalability. CMOS MEAs can achieve a higher spatial resolution and a large effective recording area by multiplexing channels onto fewer wires. However, state-of-the-art CMOS MEAs still suffer from some of the same scalability limitations. While previous work has achieved sub-cellular electrode pitch (<10μm), it can only record from a static selection of 126 electrodes simultaneously[1]. In principal, these sites can be multiplexed faster than the bandwidth of the neural signals, allowing multiple sites to be measured each sample cycle. The difficulty with high-speed multiplexing before amplification is that noise is not filtered and is therefore aliased. Conversely, reported systems with electrode-level amplification and filtering have only 256 electrodes with 200μm pitch and requires extensive post-CMOS processing[2].

Another effective way to study neural networks with MEAs is in conjunction with optical stimulation. In visual neuroscience, computer-generated patterns of light can be used to stimulate retinal photoreceptors while electrically recording activity from the ganglion cells, the retinal output. Likewise, optogenetics allows researchers to create light-sensitive cells in other biological systems to understand the way they process information. For example, neuronal cells expressing the light-reactive protein channelrhodopsin-2 can be excited optically, circumventing the need for either electrical stimulation which creates large recording artifacts, or chemical stimulation which is nonspecific[3]. Optical stimulation can be spatially and temporally precise, cell-specific, and contact-free. Therefore, optical stimulation allows researchers to control the inputs of a neural system while an MEA allows them to record multiple intermediate and output nodes of the network. While passive MEAs built on transparent substrates allow for visual correlation of electrode location, tissue, and stimulus, active MEAs on silicon substrates severely limit this capability.

Therefore, the aim of this work is provide researchers with an MEA that overcomes the limitations of both traditional passive and active MEAs for slice research. The presented MEA has a high spatial resolution, a large recording area, and integrated angle-sensitive pixels (ASP)[4] to correlate optical stimulus with recorded activity. Additionally, our array requires little post-CMOS processing for biocompatibility and can record from all sensors simultaneously.

978-1-4244-9289-3/11/$26.00 ©2011 IEEE

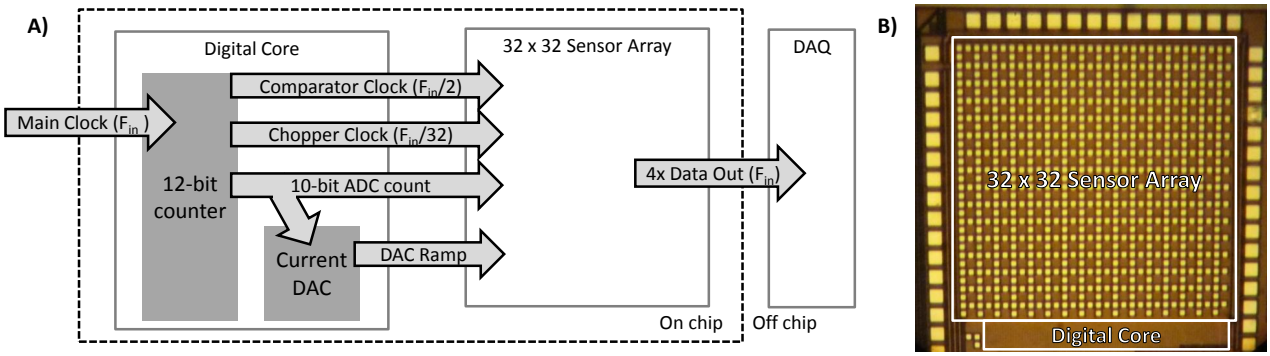

Fig. 1. **A)** System architecture of the sensor array. **B)** Die photograph of the sensory array.

II. System Design

A. System Description

The hybrid sensor array consists of 768 metal electrodes with local amplification and digitization and 2,048 photopixels. The MEA was fabricated in a standard 130nm CMOS process with an active area of 1.6mm by 1.6mm. Figure 1 shows the top level architecture of the sensor array. The only input signal is a main clock (F_{in} = 40MHz) which feeds a 12-bit counter. The counter then generates the control signals and clocks for the rest of the chip. Each sensor site is sampled at a rate of 10kHz as determined by the MSB of the counter, which is the main clock rate divided by 2^{12}. Figure 2 shows the timing diagram of the array. Sensor sampling is interleaved so that data can be output continuously at a rate equal to the main clock. There are four data output channels, each of which is fed by its own 640-bit shift register. Half of the sensors are sampled simultaneously while the other half of the sensors load and then shift data off the chip. A global 20kHz ramp signal is used as an ADC reference voltage at every sensor. The ramps is generated by a DAC built of current sources controlled by the counter with a resistive load to translate the output current into a voltage. Since control signals are generated globally, the design is highly scalable, limited by the available die area and output data rate.

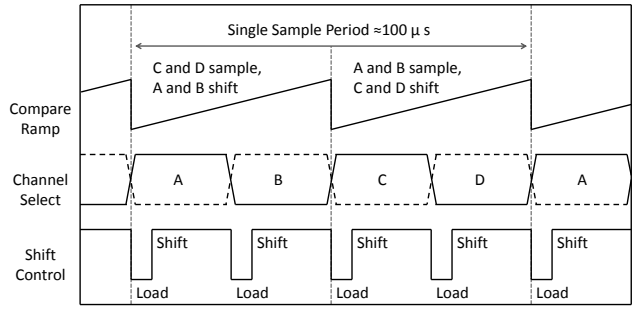

Fig. 2. Timing diagram of control signals. Half of the sensors are sampled concurrently while the other half outputs data sequentially. *Channel Select* controls the subset of sensors that are shifting data and *Shift Control* facilitates the loading and shifting of the global shift registers.

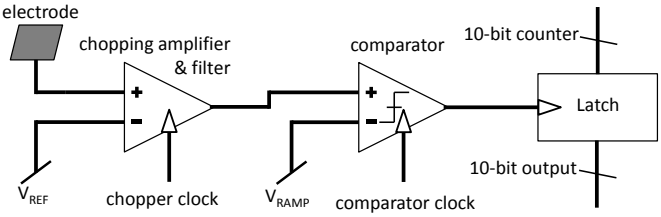

Fig. 3. Architecture of a single electrode.

B. Electrode Circuitry Design

Each electrode contains an amplifier, a switched-capacitor low-pass filter, a comparator, and a 10-bit latch as shown in Figure 3. The electrode is formed by the top metal of the CMOS metal stack and V_{REF}, common to all the amplifiers, is the applied reference potential of the electrolyte bath. Figure 4 shows a schematic of the front-end amplifier. Traditional neural amplifiers use large input transistors to reduce flicker noise and large capacitors (20pF) to block electrochemical offsets[5]. To reduce area in our design, the front-end is a folded cascode amplifier that uses chopping modulation to reduce the flicker noise of the amplifier and bias the input transistors. In simulation, the total input-referred noise voltage of our amplifier over a 10kHz bandwidth is reduced by a factor of 6.6 when chopping modulation is used. To achieve the same performance without chopping modulation, the input transistor area would need to be increased by a factor of 43.

Low-pass filtering is needed before sampling in order to prevent aliasing high frequency noise from the tissue, electrode-electrolyte interface, and the amplifier. Rather than using a large load capacitor to pull the amplifier output pole below half the sampling frequency, we used a much smaller capacitor (C_1) to suppress high-frequency chopping artifacts, followed by a switched-capacitor low-pass filter ($\omega_L = f_{chop}C_2/C_3$). This significantly decreases the required area to get the desired pole without lowering the amplifier current, which would increase thermal noise. This also allows us to control the low-pass frequency corner with the chopping frequency. The amplifier and low-pass filter occupy an area of 800μm^2, about 25 times smaller than neural amplifiers with similar performance[2].

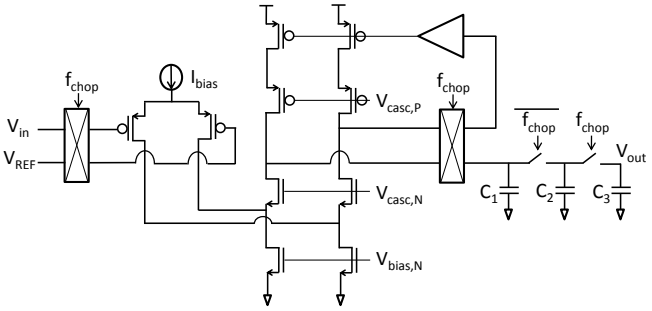

Fig. 4. Schematic of the front-end amplifier with a switched-capacitor filter.

The comparator digitizes the analog signal by comparing the amplified signal to the global ramp signal. Each step of the ramp corresponds to a 10-bit value generated by the counter in the digital core. When the ramp signal is larger than the amplified signal, the comparator clocks the latch, storing the 10-bit number locally, and then shuts down to conserve power until the next sampling cycle. The entire electrode circuitry fits within a 50μm by 45μm area (Figure 5). An additional 50μm by 5μm of each sensor site is used as part of the global shift register, which streams out the locally stored data.

C. Angle-Sensitive Pixel Design

Instead of a front-end amplifier, one-quarter of the sensor sites (*C* from Figure 5) contain eight distinct ASPs. ASPs, first introduced in [6], are devices which are sensitive to the angle of incident light and have been used to localize multiple fluorescent sources in 3D space[4]. We implemented ASPs rather than standard photopixels because they can provide a more complete description about the scattering of stimulus light in tissue. In this design, ASPs employ two local, stacked diffraction gratings on CMOS metal layers 5 and 3 directly on top of a p-implant/n-well photodiode. The lower grating is used to block or pass the periodic intensity pattern generated by light striking the top grating as a function of its lateral offset. At each sensor site there are two orientations of top diffraction grating (vertical and horizontal), and four types of bottom grating offset (0°, 90°, 180°, and 270°), for a total of eight ASP variants. Since the sampling rate needed for an ASP is much lower than an electrode, only one of the eight ASP subtypes are digitized each time for an effective sampling rate of 2.5kHz.

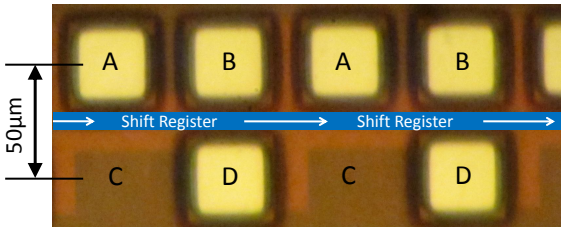

Fig. 5. Photograph of eight sensors from the main array. Subsets *A*, *B*, and *D* are electrodes and *C* is a group of ASPs. Each four-cell shares a 10-bit shift register locally, which is a portion of the global 640-bit register.

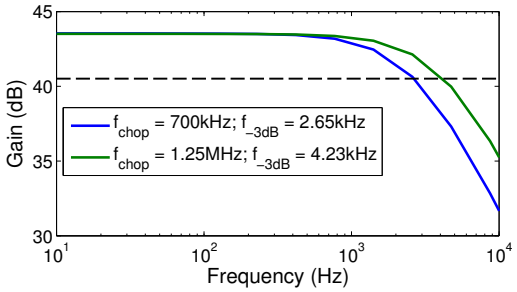

Fig. 6. Measured transfer function of the front-end amplifier with two different chopping frequencies.

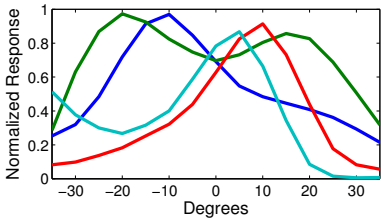

Fig. 7. Normalized angular response of four ASP subtypes with different analyzer grating offsets.

III. Experimental Results

A. System Characterization

Figure 6 shows the measured transfer function of the front-end amplifier with two different chopping frequencies. The midband gain was 43.5dB for both cases while consuming a total of 8.5μA at a supply of 1.5V. The amplifier's bandwidth changed from 4.23kHz with a 1.25MHz chopping frequency to 2.65kHz with a 700kHz chopping frequency. Note that the chopping frequency is controlled by the main clock and therefore scales with sampling rate, making the amplifier suitable for detecting action potentials at higher sampling frequencies and LFPs at lower sampling frequencies. The total measured input-referred noise was 4.1μVrms over the 4.23kHz bandwidth. The ramp ADC achieved an ENOB of 8.7 bits with a 512mV$_{pp}$ ramp, which corresponds to a resolution of 8.2μV at the input. Figure 7 shows the normalized response of four ASP subtypes to changes in incident angle. The light was generated by a green LED which was kept at a fixed distance and rotated in 5 degree increments around the sensor array.

B. Packaging

A major difficulty with using CMOS sensors is ensuring biocompatibility and protecting wirebonds from the electrolyte solution. Most post-CMOS packaging techniques use lithographically defined epoxy or patterned PDMS to encapsulate wirebonds[7]. To simplify post-processing, we encapsulated the wirebonds and defined a well around the active area using epoxy (Miller-Stephenson Epoxy 907) applied under a light microscope without a mask. The top metal of this process is aluminum, which corrodes easily[8] and is also cytotoxic[9]. To prevent the electrodes from corroding and the consequent apoptosis of the cells, we electroplated the electrodes with

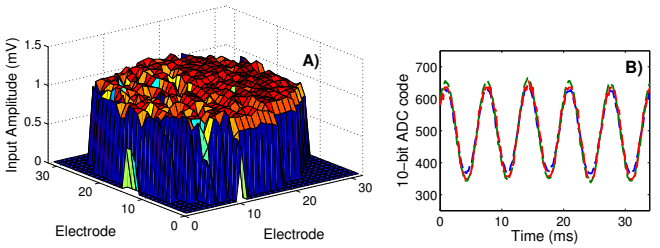

Fig. 8. **A)** Array recording of 1mV sinusiod through a silver chloride wire in aCSF with V_{REF} set to circuit ground. The voltage is the rms value of the input signal. **B)** Digitized output of three adjacent electrodes of data shown in **A**).

platinum. Platinum is nontoxic and also decreases electrode impedance. We electroplated by filling the well with a platinizing solution (chloroplatinic acid, lead acetate, hydrochloric acid). We then applied 1.5V to a platinum counter-electrode to pull current through the electrodes.

C. Measurement Results

Since each front-end amplifier operates open loop, there is a slight gain mismatch between electrodes. To calibrate and demonstrate array functionality, we filled the well with artificial cerebrospinal fluid (aCSF) and passed a 1mV sinusoid through a silver chloride wire. Figure 8A shows an uncalibrated three-dimensional map of the input-referred rms voltage recorded by the array. Figure 8B shows a 35ms overlay of three adjacent electrodes from the experiment in Figure 8A.

To confirm that our amplifiers could provide sufficiently robust, low noise recording across the full range of biologically relevant signal bands, we used them to record both LFP and spiking activity. A power spectrum of oscillatory activity from a 300μm thick mouse olfactory bulb slice is shown in Figure 9. This data, unfiltered in software, shows an oscillatory peak at the gamma band and a sharp peak at 60Hz due to line noise. Gamma oscillations are ubiquitous in the brain and are indicators of synchronous cellular activity. They arise in the olfactory bulb and change in frequency over time, resulting in a broader peak than the constant frequency line noise. More endogenous neural activity recorded from the slice is shown in Figure 10. This data was band-pass filtered in MATLAB (200Hz$\leq$f$_{bp}\leq$6kHz) to remove LFP activity. The slice was horizontally taken with a vibrating microtome. During recording, the slice was perfused in the well with oxygenated 34°C aCSF and was held down by a chrome harp with nylon netting.

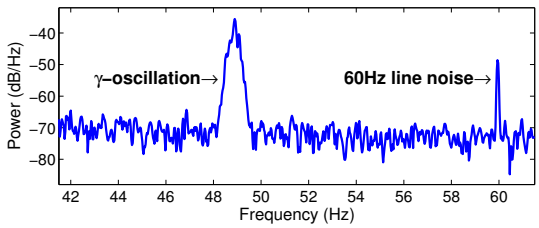

Fig. 9. Power spectrum of a long-lasting gamma oscillation in the olfactory bulb. The gamma oscillation varies in frequency over time creating a broader peak while the 60Hz line noise remains constant resulting in a narrow peak.

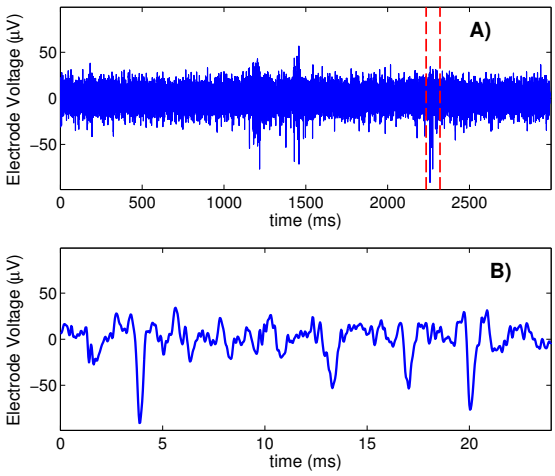

Fig. 10. **A)** A 3000ms recording of extracellular spiking activity recorded from a mouse olfactory bulb slice and a **B)** 25ms subset of **A**).

IV. Conclusion

We have presented a highly scalable architecture and demonstration of a CMOS sensor array with metal electrodes and optical sensors. Due to a distributed ADC and a compact low-noise front-end amplifier, our system achieves a high-spatial resolution of 50μm without compromising recording area or sampling rate. We also presented a simple process to encapsulate the wirebonds and to post-process the aluminum electrodes for biocompatibility. The presented system will enable unique neurophysiological experiments on a chip.

Acknowledgment

The authors would like to thank MOSIS for fabrication support and Albert Wang for ASP design assistance.

References

[1] U. Frey, F. Heer, R. Pedron, M. Ballini, J. Mueller, D. Bakkum, S. Hafizovic, F. Faraci, F. Greve, K. Kirstein, and A. Hierlemann, "Switch-matrix-based high density microelectrode array in CMOS technology," *IEEE J. Solid State Circuits*, pp. 467–482, Feb. 2010.

[2] J. Aziz, K. Abdelhalim, R. Shulyzki, R. Genov, B. Bardakjian, M. Derchansky, D. Serletis, and P. Carlen, "256-channel neural recording and delta compression microsystem with 3D electrodes," *IEEE J. Solid State Circuits*, pp. 995–1005, Mar. 2009.

[3] E. Boyden, F. Zhang, E. Bamberg, G. Nagel, and K. Deisseroth, "Millisecond-timescale, genetically targeted optical control of neural activity," *Nature Neuroscience*, pp. 1263–1268, Aug. 2005.

[4] A. Wang, P. R. Gill, and A. Molnar, "Fluorescent imaging and localization with angle sensitive pixel arrays in standard CMOS," in *Proc. of IEEE Sensors 2010*, Nov. 2010, pp. 1706–1709.

[5] R. Harrison and C. Charles, "A low-power low-noise CMOS amplifier for neural recording applications," *IEEE J. Solid State Circuits*, pp. 958–965, Jun. 2003.

[6] A. Wang, P. R. Gill, and A. Molnar, "Angle sensitive pixels in CMOS for lensless 3D imaging," in *Proc. of IEEE CICC*, Nov. 2009, pp. 371–374.

[7] M. Dandin, I. D. Jung, M. Piyasena, J. Gallagher, N. Nelson, M. Urdaneta, C. Artis, P. Abshire, and E. Smela, "Post-CMOS packaging methods for integrated biosensors," in *Proc. of IEEE Sensors 2009*, Nov. 2009, pp. 795–798.

[8] Y. Liu, E. Smela, N. Nelson, and P. Abshire, "Cell-lab on a chip: a CMOS-based microsystem for culturing and monitoring cells," in *IEEE 26th Annu. Int. Conf. EMBS*, Sep. 2004, pp. 2534–2537.

[9] S. S. A. El-Rahman, "Neuropathology of aluminum toxicity in rats (glutamate and GABA impairment)," *Pharmacological Research*, pp. 189–194, 2003.